PCCP

Accepted Manuscript

ROYAL SOCIETY OF CHEMISTRY

www.rsc.org/pccp

PCCP

ARTICLE

Effects of different manganese precursors as promoters on catalytic performance of CuO-MnO_x/TiO_2 catalysts for NO removal by CO

Received 00th April 2015,
Accepted 00th May 2015

DOI: 10.1039/x0xx00000x

www.rsc.org/

Chuanzhi Sun[a], Yingjie Tang[a], Fei Gao[b], Jingfang Sun[b], Kaili Ma[c], Changjin Tang[c], and Lin Dong[b,c]*

Two different precursors, manganese nitrate (MN) and manganese acetate (MA), were employed to prepare two series of catalysts, i.e., xCuyMn(N)/TiO_2 and xCuyMn(A)/TiO_2, by co-impregnation method. The catalysts were characterized by XRD, LRS, CO-TPR, XPS and EPR spectra. The results suggest that: (1) Both xCuyMn(N)/TiO_2 and xCuyMn(A)/TiO_2 exhibit much higher catalytic activities than unmodified Cu/TiO_2 catalyst in NO+CO reaction. Furthermore, the activities of catalysts modified with same amount of manganese are closely dependent on manganese precursors. (2) The enhancement of activities for Mn-modified catalysts should be attributed to the formation of surface synergetic oxygen vacancy (SSOV) Cu^{+}-□-Mn^{y+} in the reaction process. Moreover, since the formation of the SSOV (Cu^{+}-□-Mn^{3+}) in xCuyMn(N)/TiO_2 catalyst is easier than that (Cu^{+}-□-Mn^{2+}) in xCuyMn(A)/TiO_2 catalyst, the activity of xCuyMn(N)/TiO_2 catalyst is higher than that of the xCuyMn(A)/TiO_2 catalyst. This conclusion is well supported by the XPS and EPR results.

1 Introduction

Selective catalytic reduction of NO_x (SCR) is the most popular among other NO_x abatement technologies like storage and thermal decomposition. NO is the major component of NO_x and it is generated in combustion processes (stationary and mobile).[1, 2] The most common reductants for SCR are ammonia, urea, H_2, CO and hydrocarbons like methane, ethane and propylene. Among these methods, using carbon monoxide offers some distinct advantages compared with other reductants. Because the carbon monoxide can be produced onsite for the cases of coal or natural gas utilization (stationary sources), or it is part of the exhaust stream due to incomplete combustion of the liquid fuel (mobile sources). In this manner, one can eliminate the costly steps of purchasing, transporting and storing the reductant.[1] Thus, the NO+CO reaction was widely studied in the past years.

Use of TiO_2 as the carrier of catalysts has attracted much attention and TiO_2-based catalysts are widely applied in NO reduction.[3-5] TiO_2-based catalysts overcome the shortcoming of the deactivation arising from sulfate formation in the SO_x-containing environment, and exhibit an excellent NO conversion and N_2 selectivity. The vast majority of the catalysts reported for the NO + CO reaction are supported platinum group metals (Pt, Pd, Rh, Ir) and transition metal oxides.[6-8] Among them, copper oxides show a potential application for the abatement of exhaust gas from stationary and mobile emission sources,[9-11] thus special attention has been paid to it as a substitute for noble metal containing catalysts.

In recent years, Mn-based catalysts also attracted much attention due to its high activity for catalytic removal of NO_x. Mn-based catalysts including MnO_x, MnO_x-CeO_2, Mn/TiO_2, Mn-Fe/TiO_2, and Mn/Al-SBA-15 have been proposed as eco-friendly low temperature SCR catalysts, especially for stationary sources.[12-17] Manganese is generally recognized as a less toxic metal component compared with other metals and commonly employed for the preparation of SCR catalyst.[17] Most of the Mn-based catalysts were prepared by the impregnation method using manganese nitrate (MN) or manganese acetate (MA) as a precursor. In addition, different types of precursor (reducing organic or oxidative inorganic precursors) will induce different metal oxidation states during preparation of the catalysts, and different metal oxidation states may result in different activities of the catalysts. For example, Li et al. reported that the MN precursor resulted primarily in MnO_2, while the MA precursor caused mainly Mn_2O_3 species. In their work, the

[a] College of Chemistry, Chemical Engineering and Materials Science, Collaborative Innovation Center of Functionalized Probes for Chemical Imaging in Universities of Shandong, Key Laboratory of Molecular and Nano Probes, Ministry of Education, Shandong Provincial Key Laboratory of Clean Production of Fine Chemicals, Shandong Normal University, Jinan 250014, P. R. China.
[b] Center of Modern Analysis, Nanjing University, Nanjing 210093, P.R. China.
[c] Key Laboratory of Mesoscopic Chemistry of Ministry of Education, School of Chemistry and Chemical Engineering, Nanjing University, Nanjing 210093, P.R. China.
E-mail: donglin@nju.edu.cn Fax: 86-25-83317761

MnO_x/TiO_2 catalysts using MA as precursor exhibit higher activity for the $NO+NH_3+O_2$ reaction.[18]

In previous literature, it is reported that the binary metal oxides exhibit superior activity and N_2 selectivity for NO+CO reaction than the single ones. Mixed copper-manganese oxide has been studied extensively,[19-22] and it is proved to be high activity toward the oxidation of carbon monoxide and NO reduction by CO.[19-21] In these reactions, MnO_x species usually behaves as the promoter to improve the activity and selectivity of the catalyst.[19,20] As mentioned above, different types of precursor will induce different valences of manganese.[18] Will it take different effect as promoter? However, the effects of the different manganese precursors have been seldom examined in the previous research. In the present work, a series of $CuO-MnO_x/TiO_2$ catalysts have been prepared by co-impregnation method, and our attention was mainly focused on exploring the influence of manganese precursors (MA or MN) on the surface copper oxide and manganese oxide species and on their catalytic performance for NO removal by CO.

2 Experimental

2.1 Catalyst preparation

TiO_2 support was prepared via hydrolysis of titanium alkoxides, the product was washed, dried and then calcined in flowing air at 500 ˚C for 5 h. The anatase crystalline form of the product was identified by XRD, and the BET surface area is 56 m^2 g^{-1}.

The CuO/TiO_2, MnO_x/TiO_2 and $CuO-MnO_x/TiO_2$ catalysts were prepared by incipient-wetness impregnating on the support with the solution containing $Cu(Ac)_2$ and $Mn(NO_3)_2$ or $Mn(Ac)_2$. The CuO loading was 0.6 mmol/100 m^2 TiO_2, while the MnO_x was 0.1, 0.2, 0.4 mmol/100 m^2 TiO_2. The mixture was kept vigorously stirring for 2 h, and then evaporated at 100 ˚C. The resulting materials were dried at 110 ˚C overnight and calcined at 450 ˚C in flowing air for 4 h. These catalysts were denoted as xCu/TiO_2, $yMn(N)/TiO_2$, $yMn(A)/TiO_2$ and $xCuyMn(N\ or\ A)/TiO_2$, where the "N", "A" indicated using the $Mn(NO_3)_2$, $Mn(Ac)_2$ as precursors, ''x'' and ''y'' represented the loading amounts of copper oxides and manganese oxides, respectively.

2.2 Catalyst characterization

Brunauer-Emmet-Teller (BET) surface areas were measured by nitrogen adsorption at 77 K on a Micrometrics ASAP-2020 adsorption apparatus. Before each adsorption measurement, approximate 0.1g of a catalyst sample was degassed in a N_2/He mixture at 300 ˚C for 2 hours.

X-ray powder diffraction (XRD) patterns were collected using a Philips X'pert Pro diffractometer with Ni-filtered CuKα radiation (0.15418 nm). The X-ray tube was operated at 40 kV and 40 mA.

Raman spectra were collected on a Renishaw invia Laser Raman spectrometer using Ar^+ laser beam. The Raman spectra were recorded with an excitation wavelength of 514 nm and the laser power of 20 mW.

CO-TPR was carried out in quartz tube with a requisite quantity of catalyst (50 mg). The catalysts were pretreated in N_2 stream at 100 ˚C for 1 h and then cooled to room temperature, after that, the gas CO-He mixtures (10% CO by volume) was switched on. The CO reduction was carried out at different temperatures with a space velocity of 8000 h^{-1}. Column and thermal conduction detection were used for analyzing the production. The area of reduction peak of CO_2 was integrated to evaluate the consumption of CO.

X-ray photoelectron spectroscopy (XPS) and X-ray Auger electron spectroscopy (XAES) measurements of the *in situ* pretreated catalysts were performed on a PHI 5000 VersaProbe system, using monochromatic Al Kα radiation (1486.6 eV) operating at an accelerating power of 15 kW. The instrument used in this study has three chambers, namely (1) an ultra high vacuum (UHV) surface analysis chamber; (2) a sample transfer antechamber; and (3) a reaction chamber. The transfer antechamber is connected to both the analysis and reaction chamber. The *in situ* pretreatment was carried out in the reaction chamber. Before the measurement, the sample was further outgassed at room temperature in the UHV chamber ($< 5 \times 10^{-7}$ Pa). All binding energies (B.E.) were referenced to the Ti 2p peak at 459.3 eV. This reference gave B.E. values with an accuracy at ±0.1 eV.

Electron paramagnetic resonance (EPR) spectra were recorded on a Bruker EMX spectrometer using a 100-kHz modulation and a 4-G standard modulation width. The spectra were recorded at room temperature.

The CO pretreatment of the samples was conducted in a quartz tube. All the samples were pretreated in a flowing N_2 stream at 100 ˚C for 1 h, and heated to 400 ˚C with a ramp of 10˚C min^{-1} in the flowing N_2 stream before switch to CO. After that, the samples were exposed to CO-He mixtures (10% CO by volume) at a rate of 8.4 mL min^{-1} held for 1 h at different temperatures. The CO-pretreated samples were cooled to room temperature in the flowing N_2.

2.3 Catalytic activity tests

The activities of the catalysts were determined under steady state, involving a feed steam with a fixed composition, NO 5%, CO 10% and He 85% by volume as diluents. A quartz tube with a requisite quantity of catalyst (50 mg) was used. The catalysts were pretreated in N_2 stream at 100 ˚C for 1 h and then cooled to room temperature, after that, the gas reactants were switched on. The reactions were carried out at different temperatures with a space velocity of 12000 h^{-1}. Two columns and thermal conduction detections were used for analyzing the productions, column A with Paropak Q for separating N_2O and CO_2 , and column B, packed with 5A and 13x molecule sieve (40-60 M) for separating N_2, NO and CO.

3 Results and discussion

3.1 Catalytic activity and selectivity of NO removal by CO

Fig. 1 shows the activities and N_2 selectivities of $xCuyMn/TiO_2$ catalysts, in which a fixed copper oxide, 0.6 mmol/100 m^2 supports,

and various manganese loadings are considered. The NO+CO reactions are carried out in range of 200~350 ˚C. As can be seen, the 0.4Mn(A)/TiO_2 and 0.4Mn(N)/TiO_2 catalysts show negligible activities below 350 ˚C, while 0.6Cu/TiO_2 catalyst exhibits 5~15% in NO conversion, as shown in Fig 1(a). In addition, the activity of 0.6Cu(N)/TiO_2 catalyst is almost equal to that of the 0.6Cu(A)/TiO_2 catalyst indicating different anions (NO_3^-or Ac^-) in precursors have little influence on the activities of the Cu/TiO_2 catalysts.

Regarding all the catalysts, it can be seen that the activities of the catalysts are significantly improved when manganese oxides are introduced into the 0.6Cu/TiO_2 catalyst. Furthermore, the improvement of the activities over the 0.6CuyMn(N)/TiO_2 catalysts is much higher than that over the 0.6CuyMn(A)/TiO_2 catalysts. Compared with the 0.6Cu/TiO_2 catalyst, the activity of the 0.6Cu0.1Mn(N)/TiO_2 is improved obviously, and the NO conversion reaches about 68% at 350 ˚C. Further increase of the manganese loadings results in significant enhancement of the NO conversion, and the 0.6Cu0.4Mn(N)/TiO_2 catalyst exhibits 100% in NO conversion at 350 ˚C. However, for the 0.6CuyMn(A)/TiO_2 catalysts, the activity does not increase with the loading amounts of manganese oxides increasing. It can be seen that the activities of 0.6CuyMn(A)/TiO_2 catalysts with different manganese loadings are almost equal, and the 0.6CuyMn(A)/TiO_2 catalysts exhibit low activities with respect to 0.6CuyMn(N)/TiO_2 catalysts.

In the NO+CO reaction, the unexpected byproduct is N_2O. Fig. 1(b) shows N_2 selectivities of the catalysts. As shown in Fig. 1(b), the N_2 selectivities of all samples are relatively low when temperature is below 250 ˚C. When temperature is higher than 250˚C, the N_2 selectivities of catalysts prepared using $Mn(NO_3)_2$ as precursors are obviously enhanced. The N_2 yields profiles are given in Fig. 1(c). It can be seen that the 0.6CuyMn(N)/TiO_2 catalysts are liable to produce N_2, and the N_2 yields increase with the manganese loading amounts. However, for the 0.6CuyMn(A)/TiO_2 catalysts, the N_2 selectivities are a little improved compared with the 0.6Cu/TiO_2 catalyst. Thus, when $Mn(Ac)_2$ is used as precursors to prepare catalysts, the manganese species make smaller contribution than that of $Mn(NO_3)_2$ to the NO+CO reactivity and selectivity.

According to above results, it can be seen that single copper oxide or manganese oxide supported on TiO_2 exhibits low activities in the NO+CO reaction. Thus, the increase of the activity should be attributed to the synergetic operation between the copper oxides and manganese oxides. Furthermore, it should be noted that the synergetic operation between the copper oxides and manganese oxides is significantly affected by using the different manganese precursors. The reason for it will be investigated via the following the characterization of the catalysts.

3.2 Characterization of the catalysts

3.2.1 XRD and LRS studies of the catalysts

Fig. 2(a) shows the XRD patterns of 0.6Cu/TiO_2, 0.4Mn/TiO_2, 0.6CuyMn(N)/TiO_2 and 0.6CuyMn(A)/TiO_2 catalysts. It can be seen that only the characteristic peaks of anatase TiO_2 can be detected (JCPDS: 21-1272), without any peaks corresponding to copper oxides or manganese oxides. The results suggest that both copper oxides and manganese oxides are highly dispersed on the surface of the anatase TiO_2 support. It also demonstrates that different manganese precursors will not affect the dispersed properties of surface species. The laser-Raman spectra (LRS) experiments further confirm the XRD results (Fig. 2(b)). As can be seen, only the characteristic peaks of anatase TiO_2 appear at 147, 396, 516 and 638 cm^{-1}. No characteristic peaks of copper oxides and manganese oxides can be observed.

3.2.2 Surface species for before and after reaction of the catalysts

XPS analysis was performed for 0.6Cu/TiO_2, 0.6Cu0.4Mn(N)/TiO_2 and 0.6Cu0.4Mn(A)/TiO_2 samples before and after reaction in order to distinguish the chemical states of the surface manganese oxides and copper oxides in the reactive process, as shown in Fig. 3.

Before the NO+CO reaction (Fig. 3(a)), all the catalysts show a Cu $2p_{3/2}$ transition with a symmetric main peak (B.E. ≈ 934.2 eV), and a typical intense satellite peak appears on the higher binding energy side (B.E. ≈ 942.4 eV). The results indicate that the copper species mainly exist as +2 states before reaction (B.R.). For the 0.6Cu0.4Mn(N)/TiO_2 catalyst (Fig. 3(b)), the binding energy of Mn $2p_{3/2}$ peak appearing at about 642.5 eV should be attributed to the characteristic peak of Mn^{4+} species.[23-24] This agrees with previously reported results that the $Mn(NO_3)_2$ precursors usually decompose into MnO_2 after calcination.[18] For the 0.6Cu0.4Mn(A)/TiO_2 catalyst (Fig. 3(c)), the binding energy of the main Mn $2p_{3/2}$ peak appears at about 641.8 eV indicating the manganese species mainly exist as Mn_2O_3 initially. [23]

After the NO+CO reaction at 350 ˚C (Fig. 3(a)), the samples were also checked by XPS. For all samples, the peaks corresponding to Cu^+ species appear at about 932.3 eV and the intensity of the satellite peaks of Cu^{2+} become weaker, which indicates that part of Cu^{2+} species have been reduced to Cu^+ during the NO+CO reaction process. For the 0.6Cu0.4Mn(N)/TiO_2 catalyst (Fig. 3(b)), the peak of Mn^{4+} at 642.4 eV disappears and the main peak appears at about 641.8 eV. In addition, a satellite peak representing Mn^{2+} appears at 647.5 eV. [23] These results suggest that all Mn^{4+} species have been reduced to Mn^{3+} and Mn^{2+} in the NO+CO reaction. For the 0.6Cu0.4Mn(A)/TiO_2 catalyst (Fig. 3(c)), in addition to the Mn^{3+} species, the satellite peak of Mn^{2+} species also appears indicating part of Mn^{3+} species have been reduced to Mn^{2+}. As a result, it can be concluded that the main species in 0.6Cu0.4Mn(A)/TiO_2 catalyst are Cu^{2+}, Cu^+, Mn^{3+} and Mn^{2+} species after NO+CO reaction. Interestingly, after comparing the two samples, it can be seen that 0.6Cu0.4Mn(N)/TiO_2 catalyst contains the same species like 0.6Cu0.4Mn(A)/TiO_2 catalyst, including Cu^{2+}, Cu^+, Mn^{3+} and Mn^{2+} species. Consequently, no apparently differences can be distinguished from the perspective of types of surface ions. However, the activities of the two catalysts exhibit significant difference, and the activity of 0.6Cu0.4Mn(N)/TiO_2 catalyst is much higher than that of 0.6Cu0.4Mn(A)/TiO_2 catalyst. Thus, the increase of the activity for 0.6Cu0.4Mn(N)/TiO_2 catalyst cannot be simply attributed to the appearance of Cu^+ or Mn^{3+}/Mn^{2+} ions.

Based on above activity and XPS results, it can be concluded that a single metal oxide (CuO, Cu_2O, MnO_2, Mn_2O_3 or MnO species) should not be thought as the active species of the NO+CO reaction. The high activity of the 0.6Cu0.4Mn(N)/TiO_2 catalyst should be ascribed to other factors. So, what leads to the increase of the activity and what causes the different growth of the activity between 0.6Cu0.4Mn(A)/TiO_2 and 0.6Cu0.4Mn(N)/TiO_2 catalysts?

It is reported elsewhere,[25, 26] the copper and manganese mixed oxides ($CuMnO_x$) will form when the catalyst was prepared using co-impregnation method. Consequently, Cu-O-Mn bond should appear in the mixed oxides. Thus, we tentatively proposed that the formation of Cu-O-Mn bond may be related to the high activity of the catalyst. Considering the reduction of Cu^{2+}, Mn^{3+} and Mn^{4+} species after the CO+NO reaction, the Cu-O-Mn bond can be reduced by CO in the redox process of NO+CO reaction. Therefore, the oxygen between Cu^{2+} and Mn^{4+}/Mn^{3+} ions will be taken away forming the Cu^{x+}-□-Mn^{y+} oxygen vacancy. It is reported in the literatures that surface oxygen vacancies are active for NO reduction to N_2.[27-29] Thus, the significant enhancement of the activity may result from the formation of the Cu^{x+}-□-Mn^{y+} oxygen vacancy during the reaction process. Furthermore, the different catalytic properties of 0.6Cu0.4Mn(A)/TiO_2 and 0.6Cu0.4Mn(N)/TiO_2 catalysts may be due to the degree of difficulty for the formation of oxygen vacancies in the two samples. The surface states of oxygen vacancies can be expected by considering the surface structure of TiO_2, as discussed previously by our group.[30-32] For anatase TiO_2, the (001) plane is considered the preferentially exposed plane and the octahedral vacant sites exist in the plane, as shown in Fig. 4(a). When manganese or copper oxides is highly dispersed on the surface of TiO_2, Mn^{y+} or Cu^{2+} may occupy the surface vacant site on TiO_2, and the oxygen anions will stay at the top of the occupied site as capping oxygen, compensating the extra positive charge. A possible scheme of the surface copper and manganese species in 0.6CuyMn(N)/TiO_2 and 0.6CuyMn(A)/TiO_2 samples is shown in Fig. 4(b) and Fig. 4(c), respectively. Under the reaction atmosphere, the oxygen between the Mn^{y+} and Cu^{2+} can be taken away by CO, then the oxygen vacancy forms. Different from the oxygen vacancy offered by single surface metal oxides, it is a surface synergetic oxygen vacancy (SSOV) which forms between two different metallic ions. In our previous study,[24, 33-35] it has been reported several examples that this kind of vacancy should play a more sufficient role for NO+CO reaction. In this work, the catalytic properties of SSOV maybe closely related with the precursors of manganese, which further leads to different catalytic performances in two catalysts.

3.3 Catalytic activities of NO removal by CO and characterization of the CO-pretreated catalysts

3.3.1 Catalytic activities of NO removal by CO for CO-pretreated catalysts

In order to further support our conjecture, the catalysts are pretreated by CO at different temperatures to purposely produce surface oxygen vacancies. As the sharp increase of the activities occurs at 250 ˚C and 300 ˚C (*see section 3.1*) for the 0.6Cu0.4Mn(N)/TiO_2 and 0.6Cu0.4Mn(A)/TiO_2 catalysts, respectively, CO pretreated condition were chosen under the two temperatures. Then, the catalytic activities were tested by NO+CO reaction.

After the CO pretreatment, the activities of the NO+CO reaction over a series of catalysts were tested, as shown in Fig. 5. For the TiO_2, 0.4Mn(A)/TiO_2 and 0.4Mn(N)/TiO_2 samples, the activities are unchanged after CO pretreatment (not shown). Thus, CO pretreatment has no influence on their activities. However, for 0.6Cu/TiO_2, the NO conversions over the CO-pretreated catalysts are higher than those over the fresh catalysts. Furthermore, the influences of the CO pretreatment on the activities are also dependent on the temperature. After being pretreated at 250 ˚C, the activity of the 0.6Cu/TiO_2 sample increases in the whole temperature range. At low reaction temperatures (200 and 250 ˚C), NO conversion values on the CO-pretreated samples are near twice with respect to the fresh sample. But it is still low, only 10% in NO conversion. At high reaction temperatures (300 and 350 ˚C), NO conversion increases only about 5%. When the CO-pretreated temperature is continually increased to 300 ˚C, the activities decrease unfortunately (Fig. 5(a)). Based on these results, it can be concluded that the CO pretreatment on the 0.6Cu/TiO_2 catalyst show positive effects on the activity at low reaction temperature. However, it shows negative effects when the pretreatment is performed at high reaction temperature.

In the cases of 0.6Cu0.4Mn(A)/TiO_2 and 0.6Cu0.4Mn(N)/TiO_2 samples, the CO pretreatment shows significant effects on them. For the 0.6Cu0.4Mn(A)/TiO_2 sample, the activities increase obviously in the whole reaction temperature region after pretreated with CO at 250 ˚C. It can be seen that its maximum activity reaches about 75% at the reaction temperature of 350 ˚C. For comparison, the NO conversion is only about 40% for the fresh sample at the same temperature. Furthermore, the higher pretreatment temperature will lead to higher NO conversion. When the CO-pretreated temperature rises to 300 ˚C, the NO conversion is about four times than that of the fresh sample at the reaction temperature of 250 ˚C, and NO conversion reaches about 93% at the reaction temperature of 350 ˚C. The results suggest that the activity of 0.6Cu0.4Mn(A)/TiO_2 sample increases with the CO-pretreated temperature. For the 0.6Cu0.4Mn(N)/TiO_2 sample, after CO-pretreated at 250 ˚C, the activity of it increases in the whole reaction temperature region. Actually, when the sample is pretreated at the low reaction temperature region (≤250 ˚C), the enhancement of the activity is already quite significant. Additionally, the activity of the catalyst pretreated at 300 ˚C is almost equal to that pretreated at 250 ˚C, which suggest that the relative lower pretreatment temperature (250 ˚C) is already enough for 0.6Cu0.4Mn(N)/TiO_2 sample.

These results confirm that the CO reduction of mixed metal oxides play a very important role for the enhancement of the activity. XPS results (*see section 3.2.2*) of 0.6Cu0.4Mn(A)/TiO_2 and 0.6Cu0.4Mn(N)/TiO_2 samples have suggested that the enhancement of the activity should not be simply attributed to the appearance of low valence Cu^{x+} or Mn^{y+} ions. In addition, the increases of the activities on 0.6Cu0.4Mn(A)/TiO_2 and 0.6Cu0.4Mn(N)/TiO_2 samples

are much higher than that of 0.6Cu/TiO_2 sample. Based on these results, it seems reasonable to conclude that the formation of Cu^{x+}-□-Mn^{y+} surface synergetic oxygen vacancy (SSOV) in 0.6Cu0.4Mn(A)/TiO_2 and 0.6Cu0.4Mn(N)/TiO_2 catalysts may be responsible for the increase of the activity.

Another important phenomenon should be noted. The increase of the activities are different on 0.6Cu0.4Mn(N)/TiO_2 and 0.6Cu0.4Mn(A)/TiO_2 samples. The differences of their catalytic behaviors should be attributed to the degree of difficulty of removing the oxygen from Cu^{x+}-O-Mn^{y+} bond by CO during the extraction process in NO+CO reaction. As it can be seen in Fig. 5(b), the activity of 0.6Cu0.4Mn(A)/TiO_2 sample is closely related to the CO-pretreated temperature, and the catalyst pretreated at 300 ˚C is more active than that at 250 ˚C. This suggests that the formation of SSOV in 0.6Cu0.4Mn(A)/TiO_2 sample requires CO pretreatment at high temperature. For 0.6Cu0.4Mn(N)/TiO_2 sample, the activity of the catalyst pretreated at 250 ˚C has already been high enough. This result indicates that the SSOVs of 0.6Cu0.4Mn(N)/TiO_2 sample can be obtained via CO pretreatment under relative mild temperature. In order to further support this opinion, the CO-pretreated catalysts 0.6Cu0.4Mn(A)/TiO_2 and 0.6Cu0.4Mn(N)/TiO_2 are studied by the following characterizations.

3.3.2 Characterization of the CO-pretreated catalysts

CO-TPR is carried out to study the main reduction step of catalyst. As shown in Fig. 6, for the 0.6Cu0.4Mn(N)/TiO_2 sample, the reduction process includes three steps. The temperature from 50 ˚C to 160 ˚C mainly corresponds to the reduction of $Cu^{2+}\rightarrow Cu^{+}$, and a reduction peak appears at 150 ˚C. In the range of 190 ˚C～260 ˚C, a reduction peak presents at 237 ˚C, and this region is mainly attributed to the reduction of $Mn^{4+}\rightarrow Mn^{3+}$. When the temperature is higher than 260 ˚C, the Mn^{3+} will be reduced and the mainly reduction is $Mn^{3+}\rightarrow Mn^{2+}$. A reduction peak at 289 ˚C appears in this region. For the 0.6Cu0.4Mn(A)/TiO_2 sample, a reduction peak presents at 150 ˚C corresponding to the reduction of $Cu^{2+}\rightarrow Cu^{+}$, which is similar to the 0.6Cu0.4Mn(N)/TiO_2 sample. In addition, the reduction peak of $Mn^{3+}\rightarrow Mn^{2+}$ is also appears at 289 ˚C in 0.6Cu0.4Mn(A)/TiO_2 sample. However, no remarkable reduction peak of $Mn^{4+}\rightarrow Mn^{3+}$ appears at 237 ˚C. Thus, the results further confirm that the $Mn(NO_3)_2$ precursor leads primarily to MnO_2, while the $Mn(Ac)_2$ precursor mainly form Mn_2O_3 species. CO-TPR technique indicates the reduction of $Mn^{4+}\rightarrow Mn^{3+}$ is easier than that of $Mn^{3+}\rightarrow Mn^{2+}$. However, it is still an inaccurate technique to identify the surface species, thus the XPS was performed to study the catalyst as follows.

XPS of CO-pretreated catalysts at different operation temperature were measured to investigate the change of Cu^{x+} and Mn^{y+} species with the temperature increasing. Fig. 7 shows the Cu2p spectra of 0.6Cu0.4Mn(N)/TiO_2 and 0.6Cu0.4Mn(A)/TiO_2 samples. For 0.6Cu0.4Mn(N)/TiO_2 sample (Fig. 7(a)), at room temperature, the $Cu2p_{3/2}$ peak appears at 934.2 eV with a satellite peak at 942.4 eV, which suggests the copper species mainly exist as Cu^{2+} initially.[36, 37] With the temperature increasing to 150 ˚C, most of Cu^{2+} species are reduced to Cu^{+} and little Cu^{2+} is remained. As can be seen, the peak representing Cu^{+} appears at 932.3 eV. Further increase the temperature to 250 ˚C, no characteristic peaks of Cu^{2+} are detected suggesting all of them have been reduced to Cu^{+}. When the temperature continually increases to 300 ˚C, part of Cu^{+} species are reduced to Cu^{0}, which is inferred from the Auger LMM lines of Cu (Fig. 7(b))[38, 39]. For 0.6Cu0.4Mn(A)/TiO_2 sample (Fig. 7(c)(d)), the copper species also exist as Cu^{2+} at room temperature, and the reduction process from 150˚C to 300˚C is similar to that of 0.6Cu0.4Mn(N)/TiO_2 sample.

Fig. 8 shows the Mn2p spectra of 0.6Cu0.4Mn(N)/TiO_2 and 0.6Cu0.4Mn(A)/TiO_2 samples. As shown in Fig. 8(a), only Mn^{4+} species appear at 642.5 eV ($Mn2p_{3/2}$) and 654.3 eV ($Mn2p_{1/2}$) in the 0.6Cu0.4Mn(N)/TiO_2 sample at room temperature.[20] After CO-pretreatment at 150 ˚C, the values of the full width at half maximum (FWHM) of the $Mn2p_{3/2}$ becomes broader indicating Mn^{3+} species appear at 641.8 eV ($Mn2p_{3/2}$).[23] This result suggests that part of Mn^{4+} have been reduced to Mn^{3+}. In addition, it also suggests that the CO-TPR result ($Mn^{4+}\rightarrow Mn^{3+}$, 160˚C→260˚C) is just a rough method to judge the reduction temperature region of surface ions, because the reduction peaks of different surface species may overlap each other. With the temperature increasing to 250 ˚C, peak at 642.5 eV disappears suggesting the reduction process $Mn^{4+}\rightarrow Mn^{3+}$ is completed. Furthermore, satellite peak at 647.2 eV corresponding to Mn^{2+} appears indicating the appearance of $Mn^{3+}\rightarrow Mn^{2+}$ process.[23, 24] At the temperature of 300 ˚C, no obvious change can be observed. For the peak of $Mn2p_{3/2}$ for $Mn^{3+}$and Mn^{2+} are near, thus, it is difficult to determine whether the Mn^{3+} species has been reduced to Mn^{2+} completely. However, combined with the CO-TPR results, it can be concluded that part of Mn^{3+} still exists and is reducing at this temperature. For the 0.6Cu0.4Mn(A)/TiO_2 sample (Fig. 8(b)), only the peaks corresponding to Mn^{3+} species appear at 641.8 eV ($Mn2p_{3/2}$) and 653.2 eV ($Mn2p_{1/2}$) at room temperature. With the pretreated temperature increasing to 150 ˚C, the spectra is almost unchanged and no new species appears suggesting the Mn^{3+} species cannot be reduced by CO under this temperature. After CO pretreatment at 250 ˚C, Mn^{2+} species present with a characteristic satellite peak appearing at 647.2 eV. At the temperature of 300 ˚C, no obvious change can be observed which is similar to that of 0.6Cu0.4Mn(N)/TiO_2 sample.

Combined the XPS results in Fig. 7 and Fig. 8, it can be seen that the Cu^{2+} species are easy to be reduced by CO at 150 ˚C for both the 0.6Cu0.4Mn(N)/TiO_2 and 0.6Cu0.4Mn(A)/TiO_2 samples. However, the reduction behaviors of Mn^{x+} species are different in the two samples. As can be seen in Fig. 8(a), many of Mn^{4+} species are reduced at 150 ˚C. In other words, Mn^{4+} is reduced by CO with Cu^{2+} simultaneously in the 0.6Cu0.4Mn(N)/TiO_2 sample. Thus, it can be concluded that O^{2-} species of the surface mixed metal oxides in Cu^{2+}-O-Mn^{4+} bond can be taken away, and the Cu^{+}-□-Mn^{3+} (SSOV) can form under this temperature. Differently, for 0.6Cu0.4Mn(A)/TiO_2 sample (Fig. 8(b)), Mn^{3+} species cannot be reduced at 150 ˚C and no Cu^{+}-□-Mn^{2+} (SSOV) forms in this condition. Consequently, SSOVs is easier to form in the 0.6Cu0.4Mn(N)/TiO_2 sample than that in 0.6Cu0.4Mn(A)/TiO_2 sample. When the pretreated temperature increases to 250 ˚C,

Mn^{3+} species are reduced to Mn^{2+} (Fig. 8(b)) and Cu^{+}-□-Mn^{2+} (SSOV) can form in 0.6Cu0.4Mn(A)/TiO_2 sample correspondingly. Thus, the activities of the two samples both increase obviously after CO pretreatment at 250 ˚C. However, it should be noted that the activity of 0.6Cu0.4Mn(A)/TiO_2 sample is lower than that of 0.6Cu0.4Mn(N)/TiO_2 sample, which suggest the quantity of active sites (SSOV) is still insufficient in 0.6Cu0.4Mn(A)/TiO_2 sample as pretreated at 250 ˚C. After pretreated at 300 ˚C, more active species Cu^{+}-□-Mn^{2+} (SSOV) can be obtained and the activities of 0.6Cu0.4Mn(A)/TiO_2 sample increase continually. However, for 0.6Cu0.4Mn(N)/TiO_2 sample, enough SSOVs are obtained at 250 ˚C, thus its activities are almost unchanged although the pretreated temperature is higher. In addition, according to the XPS results in Fig. 8(a), the Mn^{3+} can be reduced to Mn^{2+} at 300 ˚C in 0.6Cu0.4Mn(N)/TiO_2 sample, and the Cu^{+}-□-Mn^{3+} will change to be Cu^{+}-□-Mn^{2+} under this condition which has no influence on its activity.

EPR is an effective measurement for the surface oxygen vacancy,[40-43] and it is employed here to characterize the catalysts. Before EPR experiments, the catalysts were firstly pretreated by CO at different temperatures, and then exposed in the air. In this process, electrons will transfer from reduced surface of catalysts to the adsorbed O_2 at the oxygen vacancy to form the O_2^- species, as shown in Fig. 9. For the 0.6Cu/TiO_2 and 0.6Cu0.4Mn(N)/TiO_2 catalyst (Fig. 9(a) (b)), no characteristic signals of O_2^- species can be observed in the fresh catalyst. After CO-pretreated at 250 ˚C, the signals of O_2^- species appear centered at g=1.997 and g=2.023, respectively. When the catalyst is CO pretreated at 300 ˚C, these signals still exist. For the fresh catalyst of 0.6Cu0.4Mn(A)/TiO_2 (Fig. 9(c)), the O_2^- species also cannot be observed. Unfortunately, signals of O_2^- species even cannot be observed at the CO-pretreated temperature of 250 ˚C, which may be attributed to the weak concentration of surface oxygen vacancies. When the pretreated temperature increase to 300 ˚C, the signals of O_2^- species appear centered at g=2.04. The different value of g for O_2^- species maybe ascribe to the different environment of vacancy. In addition, reported from the literature, the value of g for Cu^{2+} is also in the range of 2.00～2.04.[44, 45] However, it can be ascertained from the XPS results that no Cu^{2+} ions exist when the pretreated temperature is higher than 250 ˚C for all samples. Thus, it can be concluded from above results that no oxygen vacancies exist in the surface of fresh catalysts, and the CO pretreatment method will bring the oxygen vacancies for all the three catalysts.

On the basis of the literatures and our present CO-TPR, XPS and EPR results, a possible model for the formation process of surface oxygen vacancy is proposed, as shown in Fig. 10. For all samples, oxygen vacancies can be formed in the reaction process. In 0.6Cu/TiO_2 catalyst, the surface oxygen vacancy Cu^{+}-□-Cu^{+} can be formed easily (Fig. 10(a)). However, this kind of surface oxygen vacancy exhibit relative low activity which has been reported by our previous work.[24] For the manganese modified catalysts, because different manganese precursors are used, different valences of manganese ions (Mn^{4+} and Mn^{3+}) are formed on the surface of fresh sample. Consequently, the condition and steps for the formation of surface synergetic oxygen vacancies of the two kinds of catalysts are different. As shown in Fig. 10(b), the SSOV can form at low temperature due to the low reduction temperature of Mn^{4+}. Thus, the catalyst 0.6Cu0.4Mn(N)/TiO_2 exhibits good low temperature activity. However, for the 0.6Cu0.4Mn(A)/TiO_2 catalyst Fig. 10 (c), the reduction of Mn^{3+}→Mn^{2+} is hard, leading to its relative lower activity in low-temperature region (< 300 ˚C).

4 Conclusions

The present work studies the influence of manganese precursors on the catalytic performance of CuO-MnO_x/TiO_2 catalysts for NO removal by CO. Based on the above experimental results and discussion, it can be concluded that (1) Both catalysts (xCuyMn(N)/TiO_2 and xCuyMn(A)/TiO_2) are much more active than Cu/TiO_2, Mn(N)/TiO_2 and Mn(A)/TiO_2 catalysts with single active components. Moreover, the catalysts prepared using manganese nitrate (xCuyMn(N)/TiO_2) are more active than that prepared using manganese acetate (xCuyMn(A)/TiO_2), although the catalysts are modified with same amount of manganese. (2) XPS investigation is performed on 0.6Cu/TiO_2, 0.6Cu0.4Mn(N)/TiO_2 and 0.6Cu0.4Mn(A)/TiO_2 samples to confirm the valence of surface species of catalysts. Before NO+CO reaction, all copper species exist as Cu^{2+} states in all fresh catalysts. However, the valence of manganese species is closely related to the prepared manganese precursors. The manganese exists as Mn^{4+} in 0.6Cu0.4Mn(N)/TiO_2 catalyst and shows Mn^{3+} in 0.6Cu0.4Mn(A)/TiO_2 catalyst. After NO+CO reaction, Cu^{2+}, Cu^{+}, Mn^{3+} and Mn^{2+} species are all exist in the 0.6Cu0.4Mn(N)/TiO_2 and 0.6Cu0.4Mn(A)/TiO_2 catalyst, which suggest the high activity of 0.6Cu0.4Mn(N)/TiO_2 catalyst should not simply be ascribed to the Cu^{+} and Mn^{3+}/ Mn^{2+}. (3) CO pretreatment was carried out on 0.6Cu/TiO_2, 0.6Cu0.4Mn(N)/TiO_2 and 0.6Cu0.4Mn(A)/TiO_2 samples to purposely produce oxygen vacancies. The catalytic activities of NO removal by CO were evaluated, and characterization of the CO-pretreated catalysts was performed. The obtained results from XPS and EPR indicate the enhancement of activity should be attributed to the formation of Cu^{+}-□-Mn^{y+} surface synergetic oxygen vacancy (SSOV) in the reaction process. Moreover, the formation of the SSOV (Cu^{+}-□-Mn^{3+}) in xCuyMn(N)/TiO_2 catalyst is at low temperature, which is easier than that (Cu^{+}-□-Mn^{2+}) in xCuyMn(A)/TiO_2 catalyst. Thus, the activities of xCuyMn(N)/TiO_2 catalysts are higher than that of the xCuyMn(A)/TiO_2 catalysts. Our results can provide some new insights on understanding the catalytic performances of supported mixed metal oxides in NO+CO reaction.

Acknowledgements

This work was supported by National Natural Science Foundation of China (21273110, 21403134), National Basic Research Program of China (973 Program, 2010CB732300), Shandong Province Development Program of Science and Technology (2014GGX102019), and Shandong Province Advanced School Program of Science and Technology (J12LD09).

References

1 P. M. Sreekanth, P.G. Smirniotis, *Catal. Lett.*, 2008, 122, 37-42.

2 G. Busca, L. Lietti, G. Ramis, F. Berti, *Appl. Catal. B: Environ.*, 1998, 18, 1-36.

3 N. Takahashi, A. Suda, I. Hachisuka, M. Sugiura, H. Sobukawa, H. Shinjoh, *Appl. Catal. B: Environ.*, 2007, 72, 187-195.

4 C. A. Sierra-Pereira, E.A. Urquieta-González, *Fuel*, 2014, 118, 137-147.

5 Z.M. Liu, S.X. Zhang, J.H. Li, J.Z. Zhu, L.L. Ma, *Appl. Catal. B: Environ.*, 2014, 158-159, 11-19.

6 J. Nováková, L. Kubelková, *Appl. Catal. B: Environ*., 1997,14, 273-286.

7 S. Roy, N. Vegten, N. Maeda, A. Baiker, *Appl. Catal. B: Environ.*, 2012, 119-120, 279-286.

8 Z.B. Wu, B.Q. Jiang, Y. Liu, *Appl. Catal. B: Environ.*, 2008, 79, 347-355.

9 F. Boccuzzi, E. Guglielminotti, G. Martra, G. Cerrato, *J. Catal.*, 1994, 146, 449-459.

10 M.C. Wu, D.W. Goodman, *J. Phys. Chem.*, 1994, 98, 9874-9881.

11 J.W. Choung, I.S. Nam, *Appl. Catal. B: Environ*., 2006, 64, 42-50.

12 M. Kang, E.D. Park, J.M. Kim, J.E. Yie, *Appl. Catal. A: Gen*., 2007, 327, 261-269.

13 G.S. Qi, R.T. Yang, *J. Catal*., 2003, 217, 434-441.

14 P.G. Smirniotis, D.A. Pena, B.S. Uphade, *Angew. Chem. Int. Ed*., 2001, 40, 2479-2481.

15 P. Venkataswamy, K.N. Rao, D. Jampaiah, B.M. Reddy, *Appl. Catal. B: Environ*., 2015, 162, 122-132.

16 X. Liang, J.H. Li, Q.C. Lin, K.Q. Sun, *Catal. Commun*., 2007, 8, 1901-1904.

17 Y.J. Kim, H.J. Kwon, I.S. Nam, J.W. Choung, J.K. Kil, H.J. Kim, M.S. Cha, G.K. Yeo, *Catal. Today*, 2010, 151, 244-250.

18 J.H. Li, J.J. Chen, R. Ke, C.K. Luo, J.M. Hao, *Catal. Comm.*, 2007, 8, 1896-1900.

19 L.J. Liu, Q. Yu, J. Zhu, H.Q. Wan, K.Q. Sun, B. Liu, H.Y. Zhu, F. Gao, L. Dong, Y. Chen, *J. Colloid Interface Sci.*, 2010, 349, 246-255.

20 H.Q. Wan, D. Li, Y. Dai, Y.H. Hu, B. Liu, L. Dong, *J. Mol. Catal. A: Chem.*, 2010, 332, 32-44.

21 E.C. Njagi, C.H. Chen, H. Genuino, H. Galindo, H. Huang, S.L. Suib, *Appl. Catal. B: Environ.*, 2010, 99, 103-110.

22 P.M. Sreekanth, D.A. Pena, P.G. Smirniotis, *Ind. Eng. Chem. Res.*, 2006, 45, 6444-6449.

23 M.C. Biesinger, B.P. Payne, A.P. Grosvenor, L.W.M. Lau, A.R. Gerson, R.C. Smart, *Appl. Surf. Sci.*, 2011, 257, 2717-2730.

24 D. Li, Q. Yu, S.S. Li, H.Q. Wan, L.J. Liu, L. Qi, B. Liu, F. Gao, L. Dong, Y. Chen, *Chem. Eur. J*., 2011, 17, 5668-5679.

25 X.J. Tang, J.H. Fei, Z.Y. Hou, X.M. Zheng, H. Lou, *Energy & Fuels*, 2008, 22, 2877-2884.

26 M. R. Morales, B.P. Barbero, T. Lopez, A. Moreno, L. E. Cadus, *Fuel*, 2009, 88, 2122-2129.

27 Y.Y. Lv, L.C. Liu, H.L. Zhang, X.J. Yao, F. Gao, K.A.Yao, L. Dong, Y. Chen, *J. Colloid Interface Sci*., 2013, 390, 158-169.

28 H.Y. Li, S.L. Zhang, Q. Zhong, *J. Colloid Interface Sci*., 2013, 402,190-195.

29 Y. Wang, A.M. Zhu, Y.Z. Zhang, C.T. Au, X.F. Yang, C. Shi, *Appl. Catal. B: Environ*., 2008, 81, 141-149.

30 C.Z. Sun, J. Zhu, Y.Y. Lv,, L. Qi, B. Liu, F. Gao, K.Q. Sun, L. Dong, Y. Chen, *Appl. Catal. B: Environ*., 2011, 103, 206-220.

31 B. Xu, L. Dong, Y. Chen, *J. Chem. Soc*., *Faraday Trans*., 1998, 94 (13) 1905-1909.

32 H.Y. Zhu, M.M. Shen, Y. Kong, J. Hong, Y. Hu, T. Liu, L. Dong, Y. Chen, C. Jian, Z. Liu, *J. Mol. Catal. A: Chem*., 2004, 219, 155-164.

33 Y.Y. Lv, H.L. Zhang, Y. Cao, L.H. Dong, L.L. Zhang, K. Yao, F. Gao, L. Dong, Y. Chen, *J. Colloid Interface Sci*., 2012, 372,63-72.

34 X.J. Yao, C.J. Tang, F. Gao, L. Dong, *Catal. Sci. Technol.*, 2014, 4, 2814-2829.

35 Y. Xiong, X.J. Yao, C.J. Tang, L. Zhang, Y. Cao, Y. Deng, F. Gao, L. Dong, *Catal. Sci. Technol.*, 2014, 4, 4416-4425.

36 J. Papavasiliou, G. Avgouropoulos, T. Ioannides, *J. Catal*., 2007, 251, 7-20.

37 T. Mathew, N. R. Shiju, K. Sreekumar, B. S. Rao, C. S. Gopinath, *J. Catal.*, 2002, 210, 405-417.

38 Y. Tanaka, R. Kikuchi, T. Takeguchi, K. Eguchi, *Appl. Catal. B: Environ.*, 2005, 57, 211-222.

39 J.P. Espinós, J. Morales, A. Barranco, A. Caballero, J.P. Holgado, A.R. González-Elipe, *J. Phys. Chem. B*, 2002, 106, 6921-6929.

40 A. Martínez-Arias, D. Gamarra, M. Fernández-García, X.Q. Wang, J.C. Hanson, J.A. Rodriguez, *J. Catal.,*2006, 240, 1-7.

41 L.H. Dong, L.L. Zhang, C.Z. Sun, W.J. Yu, J. Zhu, L.J. Liu, B. Liu, Y.H. Hu, F. Gao, L. Dong, Y. Chen, *ACS Catal.*, 2011, 1, 468-480.

42 J. Green, E. Carter, D. M. Murphy, *Chem. Phys. lett.*, 2009, 477, 340-344.

43 Z.Z. Zhang, X.X. Wang, J.L. Long, Gu Q., Z.X. Ding, X.Z. Fu, *J. Catal.*, 2010, 276, 201-214.

44 M. Karthik, H.L. Bai, *Appl. Catal. B: Environ*., 2014, 144, 809-815.

45 Z. Wang, Z.P. Qu, X. Quan, Z. Li, H. Wang, R. Fan, *Appl. Catal. B: Environ*., 2013, 134-135, 153-166.

Figures

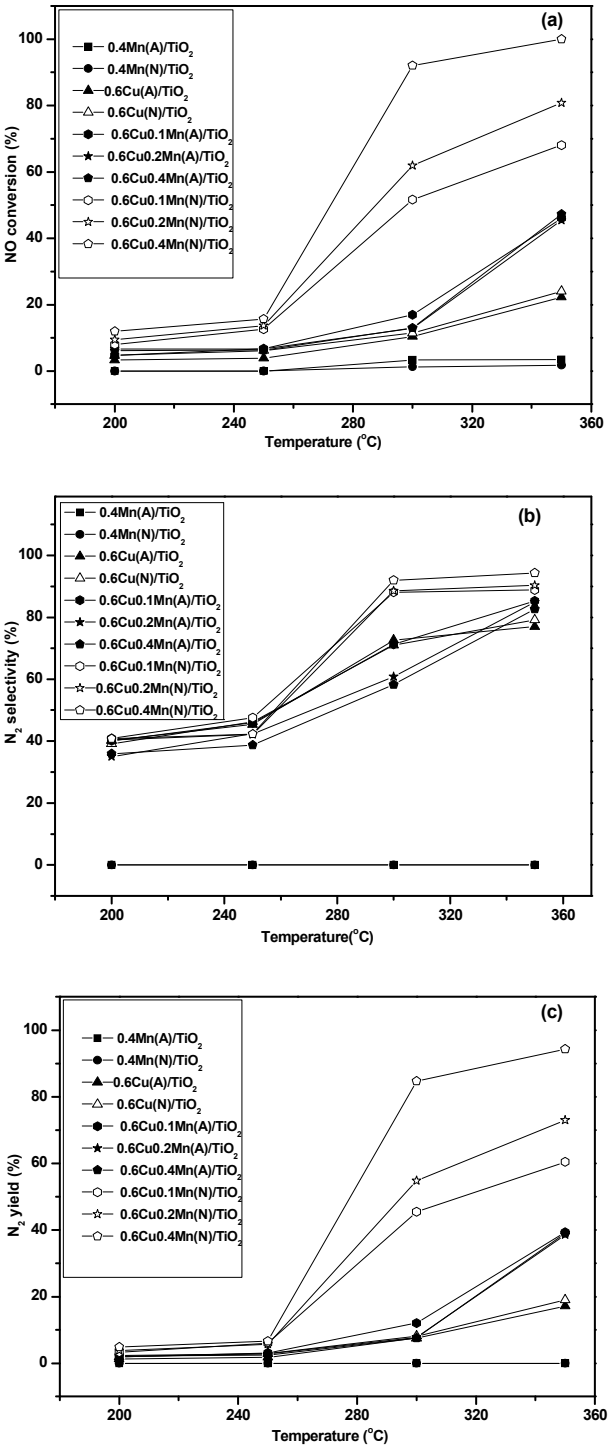

Fig. 1 The (a) NO conversions, (b) N_2 selectivities and (c) N_2 yields of xCuyMn/TiO_2 catalysts

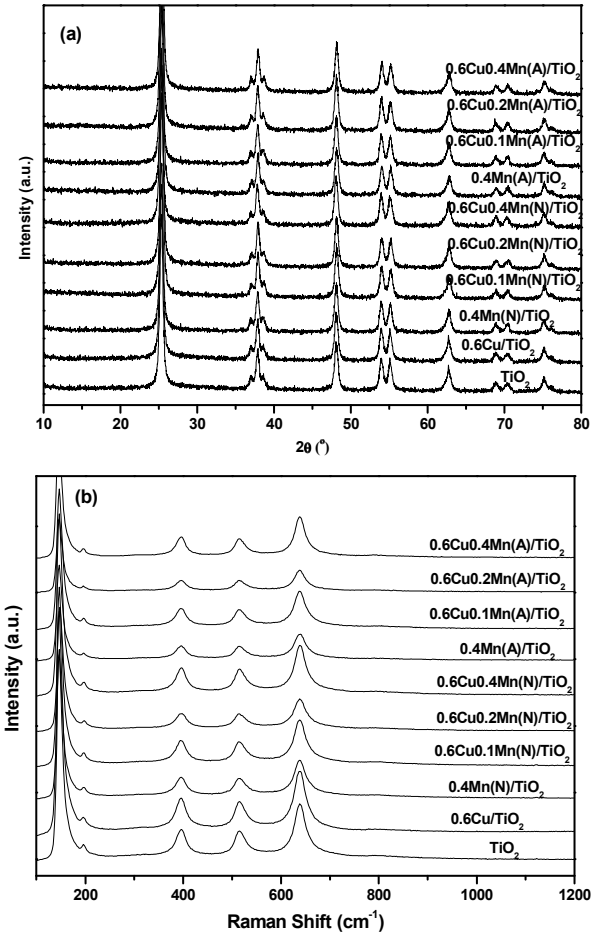

Fig. 2 The (a) XRD and (b) LRS patterns of TiO_2, 0.6Cu/TiO_2, 0.4Mn(N)/TiO_2, 0.6Cu0.1Mn(N)/TiO_2,0.6Cu0.2Mn(N)/TiO_2, 0.6Cu0.4Mn(N)/TiO_2, 0.4Mn(A)/TiO_2 0.6Cu0.1Mn(A)/TiO_2, 0.6Cu0.2Mn(A)/TiO_2, 0.6Cu0.4Mn(A)/TiO_2

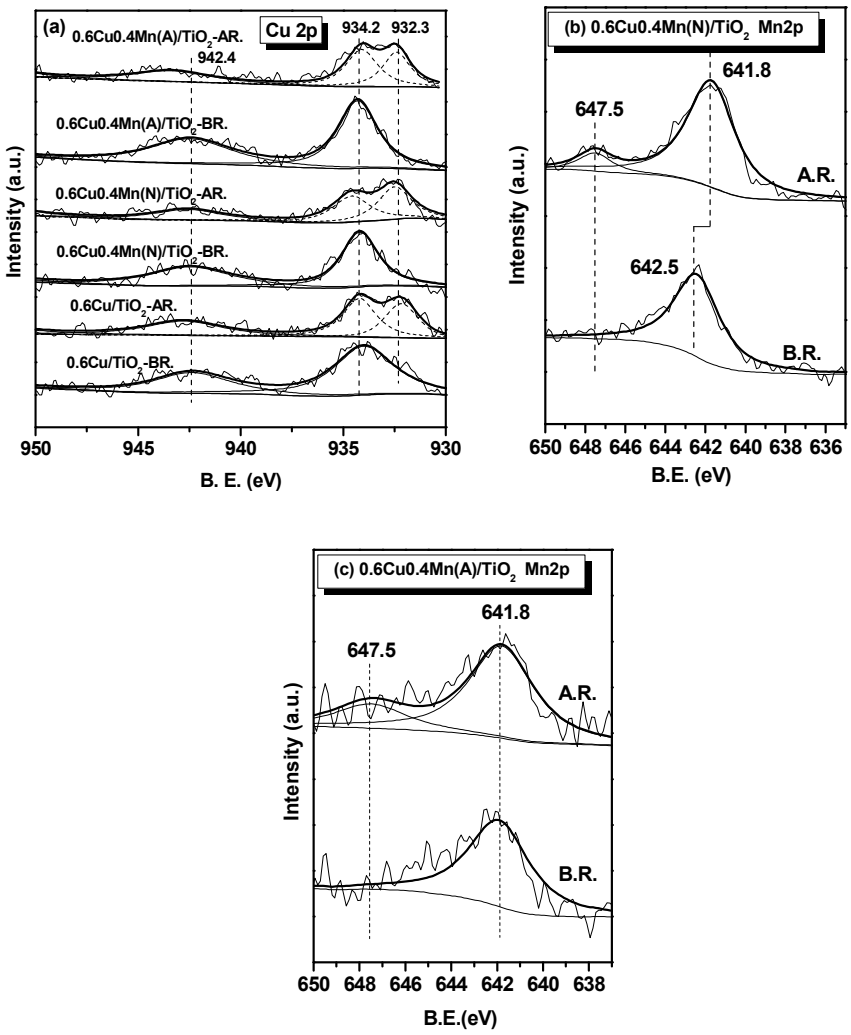

Fig. 3 XPS results for 0.6Cu/TiO_2, 0.6Cu0.4Mn(N)/TiO_2 and 0.6Cu0.4Mn(A)/TiO_2 samples before (B.R.) and after reaction (A.R.).

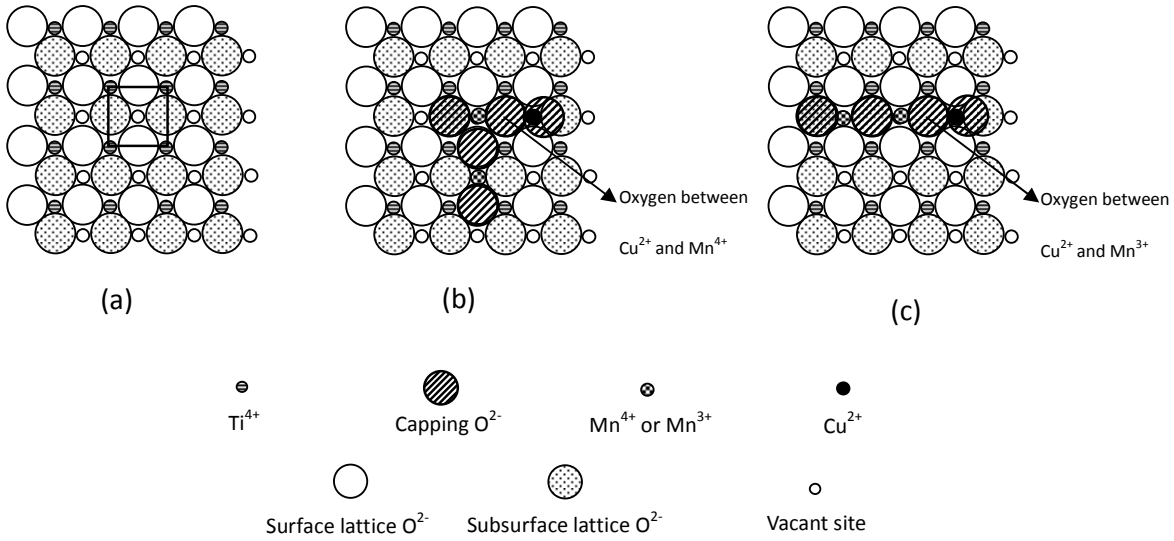

Fig. 4 The schematic diagram for the incorporated Cu^{2+} and Mn^{x+} ions in the surface vacant sites on the (001) plane of TiO_2 (anatase).

PCCP

ARTICLE

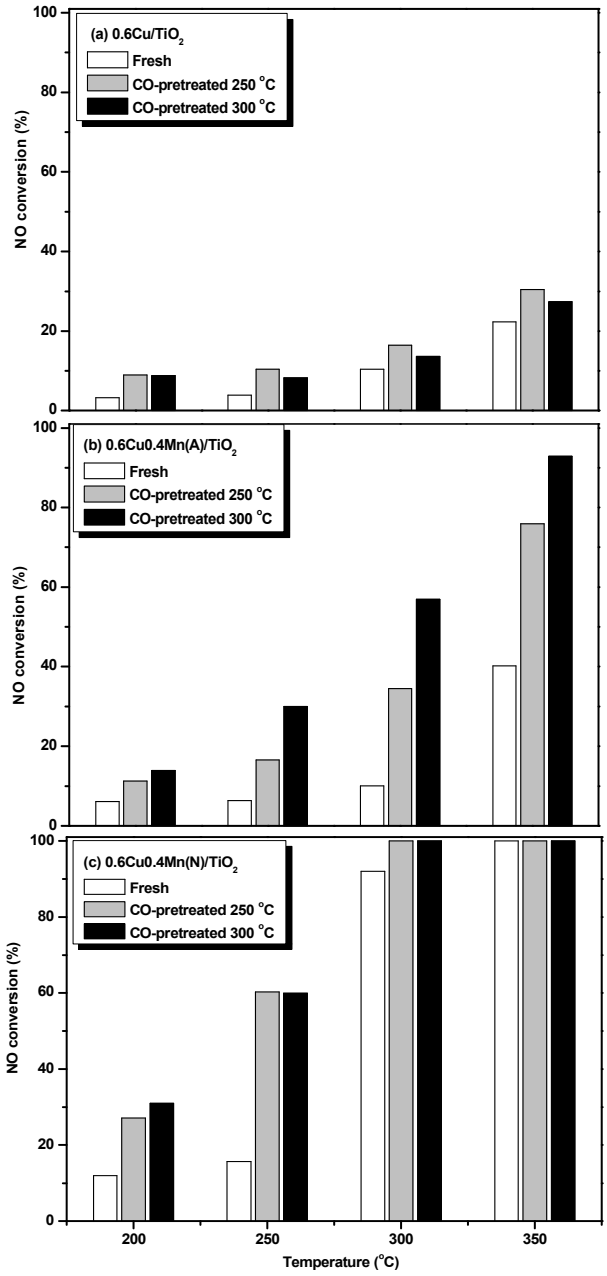

Fig. 5 The activities of the NO+CO reaction over the fresh and CO-pretreated catalysts (a) 0.6Cu/TiO_2, (b) 0.6Cu0.4Mn(A)/TiO_2 and (c) 0.6Cu0.4Mn(N)/TiO_2

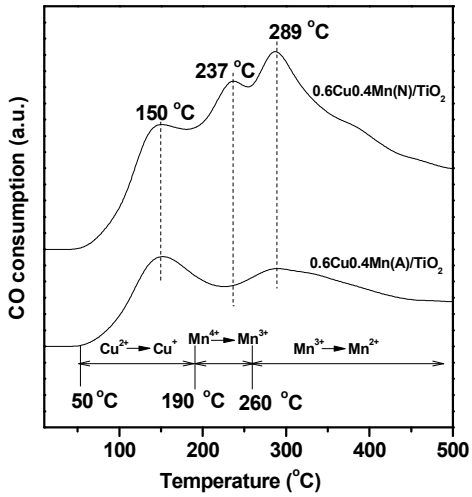

Fig. 6 CO temperature programmed reduction (TPR) of the 0.6Cu0.4Mn(N)/TiO_2 and 0.6Cu0.4Mn(A)/TiO_2 samples

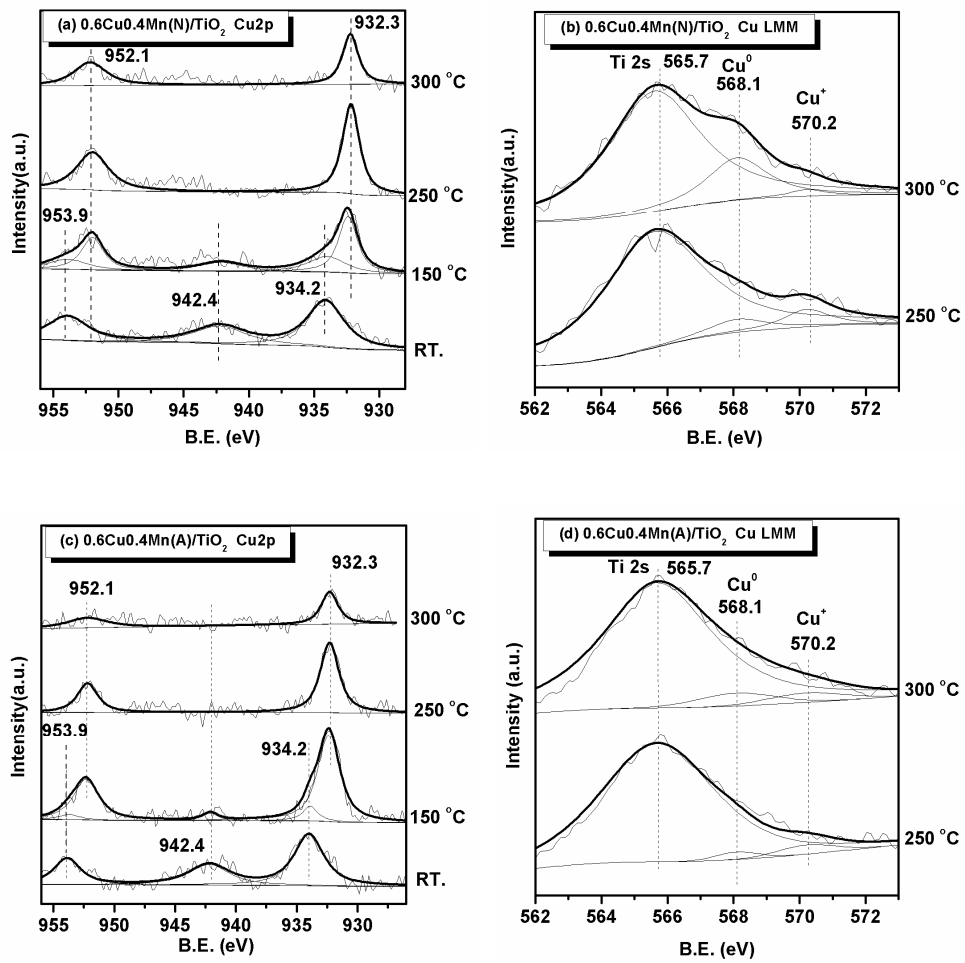

Fig. 7 The (a) Cu2p and (b) Cu-LMM spectra of CO-pretreated 0.6Cu0.4Mn(N)/TiO_2; (c) Cu2p and (d) Cu-LMM spectra of CO-pretreated 0.6Cu0.4Mn(A)/TiO_2

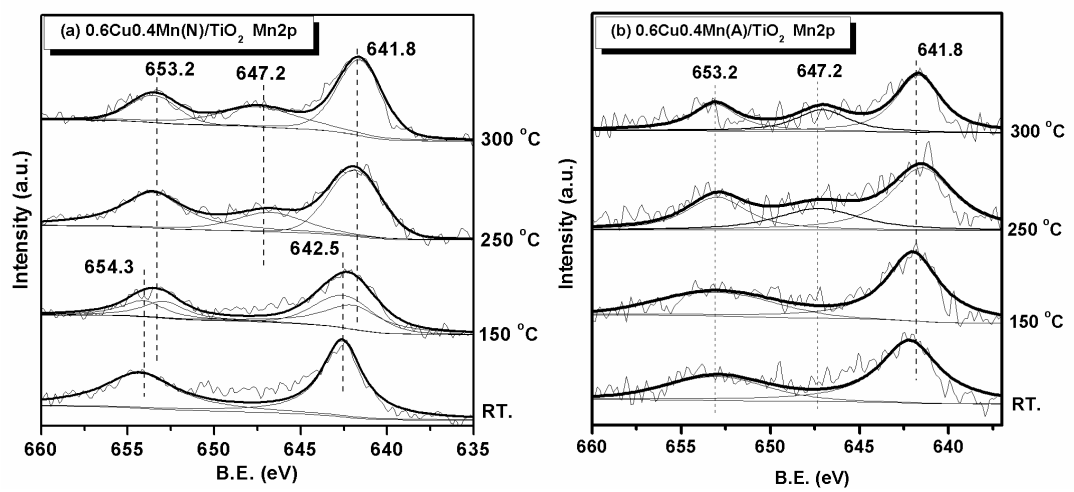

Fig. 8 The Mn2p spectra of (a) CO-pretreated 0.6Cu0.4Mn(N)/TiO_2 and (b) CO-pretreated 0.6Cu0.4Mn(A)/TiO_2

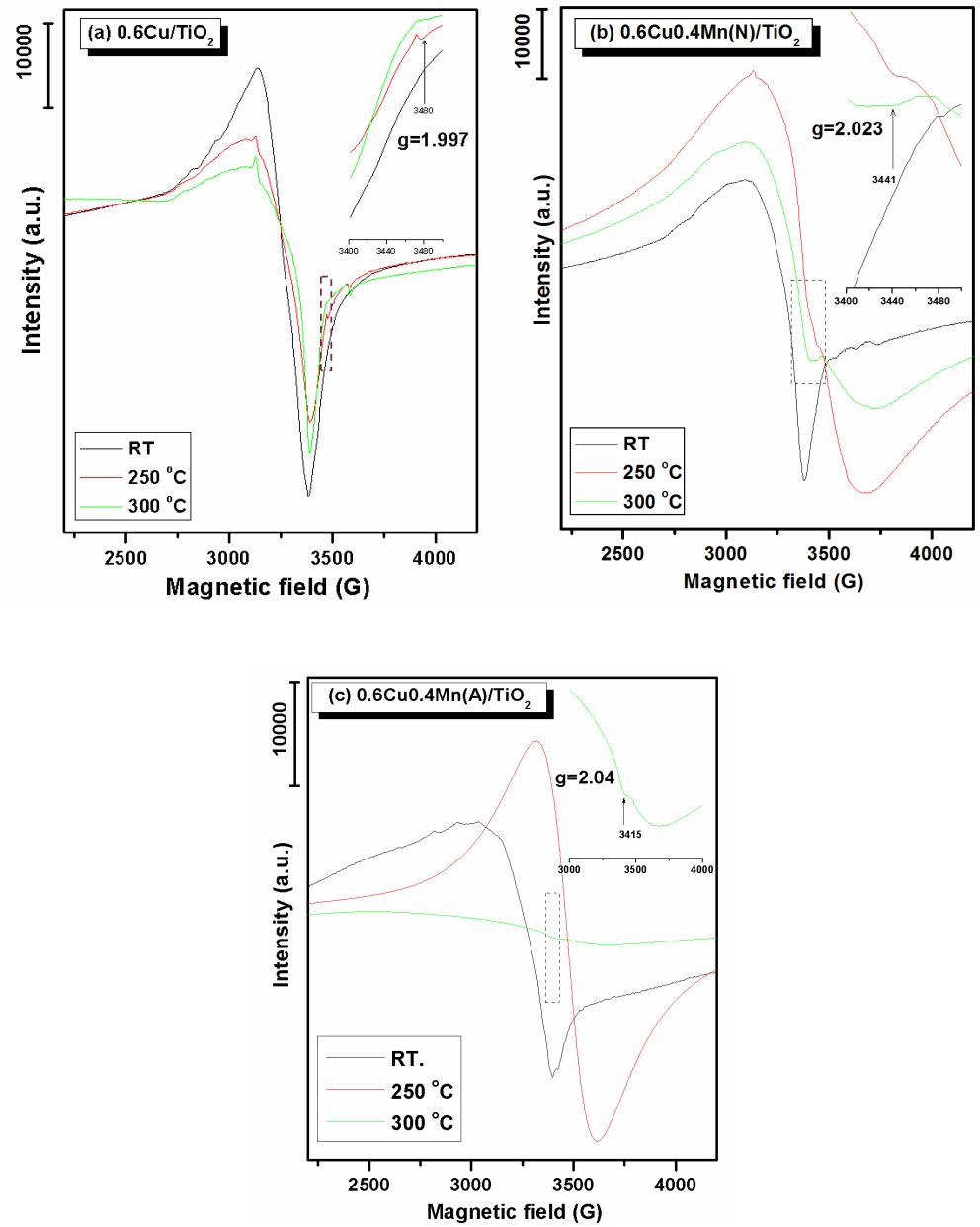

Fig. 9 EPR spectra of (a) 0.6Cu/TiO_2; (b) 0.6Cu0.4Mn(N)/TiO_2; (c) 0.6Cu0.4Mn(A)/TiO_2 catalyst

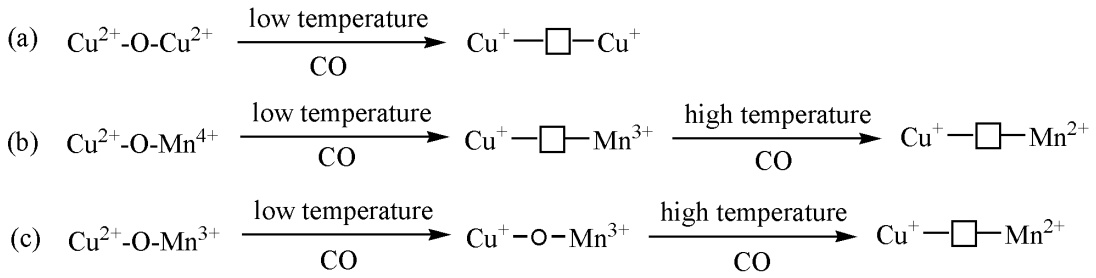

Fig. 10 Possible model for the formation process of surface oxygen vacancy (a) 0.6Cu/TiO_2; (b) 0.6Cu0.4Mn(N)/TiO_2; (c) 0.6Cu0.4Mn(A)/TiO_2 catalysts

